Wastewater Surveillance to Confirm Differences in Influenza A Infection between Michigan, USA, and Ontario, Canada, September 2022–March 2023

Ryland Corchis-Scott, Mackenzie Beach, Qiudi Geng, Ana Podadera, Owen Corchis-Scott, John Norton, Andrea Busch, Russell A. Faust, Stacey McFarlane, Scott Withington, Bridget Irwin, Mehdi Aloosh, Kenneth K.S. Ng, R. Michael McKay

Wastewater surveillance is an effective way to track the prevalence of infectious agents within a community and, potentially, the spread of pathogens between jurisdictions. We conducted a retrospective wastewater surveillance study of the 2022–23 influenza season in 2 communities, Detroit, Michigan, USA, and Windsor-Essex, Ontario, Canada, that form North America's largest cross-border conurbation. We observed a positive relationship between influenza-related hospitalizations and the influenza A virus (IAV) wastewater signal in Windsor-Essex ($\rho = 0.785$; $p<0.001$) and an association between influenza-related hospitalizations in Michigan and the IAV wastewater signal for Detroit ($\rho = 0.769$; $p<0.001$). Time-lagged cross correlation and qualitative examination of wastewater signal in the monitored sewersheds showed the peak of the IAV season in Detroit was delayed behind Windsor-Essex by 3 weeks. Wastewater surveillance for IAV reflects regional differences in infection dynamics which may be influenced by many factors, including the timing of vaccine administration between jurisdictions.

The SARS-CoV-2 pandemic reasserted the importance of epidemic preparedness and surveillance systems for infectious diseases (*1*). Informed responses to public health challenges require that data be available to decision-makers in a timely manner for early interventions (*1*). However, traditional clinical based measures of disease incidence have limited use in providing early warnings. Relying on influenza-like illness data is problematic because of difficulty distinguishing between infections ascribed to influenza A virus (IAV), influenza B virus, SARS-CoV-2, or respiratory syncytial virus (*2*). Virologic surveillance enables respiratory illness to be classified on the basis of etiologic agent. However, results are often slow, and interpretation must account for factors such as test-seeking behavior, accessibility of healthcare services, severity of infection, diagnostic practices of healthcare providers, and hospital protocols. In addition, laboratory capacity may be exceeded, and testing is expensive (*3*,*4*).

Wastewater surveillance (WS) is shown to be a practical approach for disease surveillance at various spatial scales, offering effectiveness and economic advantage (*5*,*6*). WS for SARS-CoV-2 relies on quantifying viral RNA shed in feces and has substantially increased in use since its implementation to track infections during the COVID-19 pandemic. Studies have found the concentration of SARS-CoV-2 RNA in municipal sewage covaries with the levels of disease circulating within the community served and can predict trends in clinical cases and hospitalizations (*7*,*8*). In addition, WS has the potential to be rapid; sample

Author affiliations: University of Windsor, Windsor, Ontario, Canada (R. Corchis-Scott, M. Beach, Q. Geng, A. Podadera, O. Corchis-Scott, K.K.S. Ng, R.M. McKay); Great Lakes Water Authority, Detroit, Michigan, USA (J. Norton, A. Busch); Oakland County Health Division, Oakland, Michigan, USA (R.A. Faust); Macomb County Health Department, Macomb, Michigan, USA (S. McFarlane); Detroit Health Department, Detroit (S. Withington);Windsor-Essex County Health Unit, Windsor (B. Irwin, M. Aloosh); McMaster University, Hamilton, Ontario (M. Aloosh)

DOI: https://doi.org/10.3201/eid3008.240225

processing, measurement, analysis, and dissemination of results took <6 hours in Windsor-Essex, Ontario, Canada. Calls have been made to expand the scope of WS to include monitoring of IAV and other endemic respiratory pathogens that are underreported (*9*,*10*). Similar to SARS-CoV-2, IAV can be shed in feces (*11*), and recent studies have used WS to track IAV (*12*–*14*). However, more work needs to be done to validate WS compared with traditional surveillance metrics. WS can be useful in measuring regional differences in infection dynamics and understanding how IAV and other pathogens spread across jurisdictional boundaries.

The Detroit-Windsor metropolitan area, encompassing the cities of Detroit, Michigan USA, and Windsor-Essex, Ontario, Canada, is North America's largest transborder conurbation and is the busiest cross-border region for trade between the United States and Canada, handling 42% of commercial traffic between Ontario and Michigan and accounting for ≈25% of total daily commercial traffic between the United States and Canada (*15*). The region is a major entry point for visitors, including >5,000 commuters from Windsor-Essex who cross the border daily for work (*15*,*16*). Detroit and Windsor-Essex represent government structures and public health jurisdictions that adopted fundamentally different vaccination and mitigation strategies during the COVID-19 pandemic. The cessation of COVID-19 pandemic mitigation strategies, such as masking and social distancing, affected the circulation of respiratory pathogens other than SARS-CoV-2, such as IAV. The end of those mitigation strategies resulted in a delayed start to the 2021–22 influenza season in Windsor-Essex, which coincided with the removal of mask mandates in Ontario in March 2022, and may have had a role in unusual patterns of influenza incidence during the 2022–23 influenza season in Canada (*17*,*18*). Similarly, the 2021–22 influenza season in Michigan was mild, with an increase in influenza activity observed in November, followed by a decline in January 2022 and a subsequent rise in activity in March 2022. Trends in Michigan were similar to national trends; levels of influenza activity remained elevated through mid-June 2022 (*19*,*20*). Those unusual patterns of influenza prompted this retrospective investigation comparing the incidence of influenza in Windsor-Essex with the incidence of influenza in Detroit. Our goal is to understand how jurisdictional differences in pandemic mitigation strategies and public health policy influenced the timing of influenza seasons.

The initial investigation into influenza hospitalization data for Windsor-Essex and Michigan through a visual inspection of the data showed a delay in the onset and peak of the 2022–23 influenza season in Michigan compared with Windsor-Essex. Because influenza incidence data (including hospitalizations) specific to Detroit are not publicly available and influenza is an underreported disease, the trend observed through examination of clinical data may not be sufficient to claim a delayed onset in the influenza season. Because WS is based on the aggregated waste of an entire community, it is anonymous and reflects population level trends that could produce a more sensitive and non-biased measure of influenza incidence to confirm trends in clinical data. Analysis of WS data, coupled with traditional measures of disease incidence, will enable a more complete understanding of how differences in public health approaches in a divided, yet contiguous, metropolitan area influenced the trajectory of the influenza season after COVID-19 mitigation policy removal.

Methods

Sample Collection

During September 1, 2022–March 31, 2023, we collected composite (24-h) wastewater samples 3–5 days/week from 2 different wastewater treatment plants that serve a resident population of ≈270,000 persons, ≈50% of the regional population, located in Windsor-Essex. In parallel, we collected composite samples 1 day/week from the 3 interceptors terminating at the Water Resource Recovery Facility (WRRF) operated by the Great Lakes Water Authority (GLWA), located in Detroit (*21*) (Appendix, https://wwwnc.cdc.gov/EID/article/30/8/24-0225-App1.pdf). The WRRF serves the entire city of Detroit and treats the waste of ≈3 million people, 88% of the residents in the greater Detroit metropolitan area and approximately one third the population of Michigan (*22*).

Sample Processing

We concentrated composite samples of raw wastewater by using filtration, then extracted RNA from the filters (Appendix). We used quantitative reverse transcription PCR (qRT-PCR) to measure the concentration of IAV in wastewater samples (Appendix). The assay targeted RNA coding for the matrix protein 1 (M1) of IAV by using primers and probes developed by the Centers for Disease Control and Prevention (*23*). We used a synthetic influenza H3N2 RNA (Twist Bioscience, https://www.twistbioscience.com) as a standard for comparison. We conducted qRT-PCR to measure the levels of pepper mild mottle virus (PMMoV) within the wastewater (Appendix); PMMoV

can indicate the presence of human fecal matter and is used to account for variability in wastewater flow or other physicochemical parameters influencing viral RNA concentration (*24*). We sequenced select IAV amplicons produced through qRT-PCR of RNA extracted from wastewater to validate the identity of the target (Appendix).

Clinical Data

We obtained influenza hospitalization data for Windsor-Essex through collaboration with the Windsor-Essex County health unit. Using IntelliHealth (https://intellihealth.moh.gov.on.ca) on April 17, 2024, we extracted data from the discharge abstract database and included hospitalization data from September 2022–March 2023. Influenza hospitalizations included hospital admissions where the main diagnoses had a code of J09, J100, J101, J108, J110, J111, or J118 from the International Classification of Diseases, 10th Revision. Windsor-Essex hospitalization data captured all local hospitalizations and included hospitalizations among all residents of Windsor-Essex County, regardless of where the hospitalization occurred. We aggregated influenza hospitalizations by epidemiologic week of initial admission and used hospitalizations per 100,000 persons in subsequent analysis.

We collected influenza-related hospitalization data for Michigan from the Centers for Disease Control and Prevention's influenza hospitalization surveillance network (FluSurv-NET), which records laboratory-confirmed influenza-associated hospitalizations during the influenza season as cases per 100,000 persons. We defined influenza-related hospitalization rates as the number of hospitalized persons who tested positive for influenza, of any subtype, through laboratory testing within the 14 days before or during hospitalization (*25*). Hospitalization data were available beginning in October 2022. Although hospitalization data were only available for Clinton, Eaton, Genesee, Ingham, and Washtenaw counties, those data are considered a statewide assessment of influenza for Michigan. Because the WRRF serves approximately one third of the state population, influenza-related hospitalization trends are likely to be reflected in IAV RNA concentrations at the WRRF.

Data Analysis and Visualization

We used R version 4.3.2 (The R Foundation for Statistical Computing, https://www.r-project.org) for data analysis, including the calculations of Kendall rank correlation coefficient (τ), Spearman rank correlation coefficient (ρ), nonparametric measures of correlation, and nonparametric time lagged cross correlation (TLCC) by using the ccf_boot function in the R package funtimes (Functions for Time Series Analysis, https://cran.r-project.org/web/packages/funtimes). We used Veusz version 3.6.2 (https://veusz.github.io) for data visualization. By using a population-weighted mean, we combined IAV and PMMoV RNA concentration measurements from Windsor-Essex wastewater treatment facilities. We then used downsampling through blockwise averaging to condense the data into a single measurement for each epidemiologic week; this process produced equally spaced data and enabled comparison with hospitalization data available in weekly reports (*26*). Blockwise averaging was not possible for IAV and PMMoV RNA concentration measurements of samples collected from the GLWA-WRRF because samples were collected weekly. No samples were collected from GLWA-WRRF interceptors during epidemiologic week 40 (October 2–8, 2022) and 48 (November 27–December 3, 2022). We filled in the data from epidemiologic weeks 40 and 48 by using linear interpolation before analysis. We used a population-weighted mean to combine the IAV and PMMoV signal for the 3 interceptors that discharge to the GLWA-WRRF, which produced 31 measurements of IAV RNA and 31 measurements of PMMoV RNA concentration for Detroit. All gene concentrations are reported as gene copies (gc) per liter. We produced normalized values for the IAV signal by taking the ratio of IAV M1 gene concentration to the concentration of PMMoV.

We used TLCC with Spearman rank correlations to determine if IAV wastewater signals were leading or lagging indicators of influenza-associated hospitalizations in Windsor-Essex and Michigan. TLCC relies on correlations between data series shifted relative to each other in time and can identify peak synchrony. We determined peak synchrony by the shift that produced the highest Spearman rank correlation coefficient between the 2 timeseries. We also used TLCC to compare the IAV wastewater signal in Windsor-Essex to the IAV wastewater signal in Detroit. We verified the nonnormal data by examining the quantile-quantile plots. We used nonparametric means of correlation, including Kendall rank correlation coefficient and Spearman rank correlation coefficient, to quantify the association between the IAV signal in the wastewater and influenza hospitalizations in both Windsor and Detroit. Correlations between influenza-related hospitalizations and wastewater signal in Detroit were based on 26 weeks of data because hospitalization data were not available until October 2022.

Results

IAV M1 Gene Concentrations in Windsor-Essex

Trends in IAV M1 gene concentrations at the monitored plants visually matched trends in influenza-associated hospitalizations in Windsor-Essex for September 2022–March 2023 (Figure). The TLCC for Windsor-Essex showed that wastewater signal lagged new hospital admissions on an epidemiologic week basis (Table 1) and therefore did not provide lead-time. We observed a strong positive relationship between influenza-associated hospitalizations and the population-weighted mean IAV M1 gene concentration ($\tau = 0.650$, $p<0.001$; $\rho = 0.785$, $p<0.001$) (Table 2). Signal normalization with PMMoV RNA concentrations did not improve the association between wastewater signal and influenza-associated hospitalizations ($\tau = 0.754$, $p<0.001$; $\rho = 0.630$, $p<0.001$) or change peak synchrony (Tables 1, 2).

IAV M1 Gene Concentrations in Detroit

IAV M1 gene concentrations for metro Detroit closely matched the number of new influenza-related hospitalizations in Michigan from October 2022–March 2023 (Figure). We observed a strong positive relationship between influenza-related hospitalizations and the population-weighted mean IAV M1 gene concentration for Detroit ($\tau = 0.616$, $p<0.001$; $\rho = 0.769$, $p<0.001$) (Table 3). The nonparametric TLCC results showed the IAV wastewater signal from Detroit neither lagged nor led influenza-related hospitalizations in the state of Michigan, suggesting the IAV wastewater signal is concordant with influenza-related hospitalizations (Table 1; Figure). Normalization of IAV M1 gene concentrations with PMMoV RNA concentrations did not change the degree of association between the wastewater signal and influenza-related hospitalizations for Michigan ($\tau = 0.559$, $p<0.001$; $\rho = 0.708$, $p<0.001$) or change peak synchrony (Tables 1, 3).

Cross-Border Comparison of WS for IAV

The onset and peak of the 2022–23 IAV wastewater signal in Windsor-Essex was observed before the onset and peak of the IAV wastewater signal in Detroit (Figure). TLCC using Spearman rank correlations between the population-weighted weekly average of M1 gene concentrations in Detroit and Windsor-Essex showed the 2022–23 IAV wastewater signal in Detroit lagged the corresponding IAV wastewater signal in Windsor by ≈3 weeks (Table 1). Further comparison by using PMMoV-normalized, population-weighted, weekly averages of the wastewater signal corroborated the lag of ≈3 weeks between Windsor-Essex and Detroit (Table 1).

Discussion

Our study builds on a growing body of evidence that WS for IAV is highly concordant with the results of other disease incidence measures (*13*,*28*). During the 31-week period of retrospective analysis, influenza-related hospitalizations within Windsor-Essex and Michigan covaried with the concentration of IAV RNA measured in wastewater. However, the IAV signal was not a leading indicator of influenza incidence in

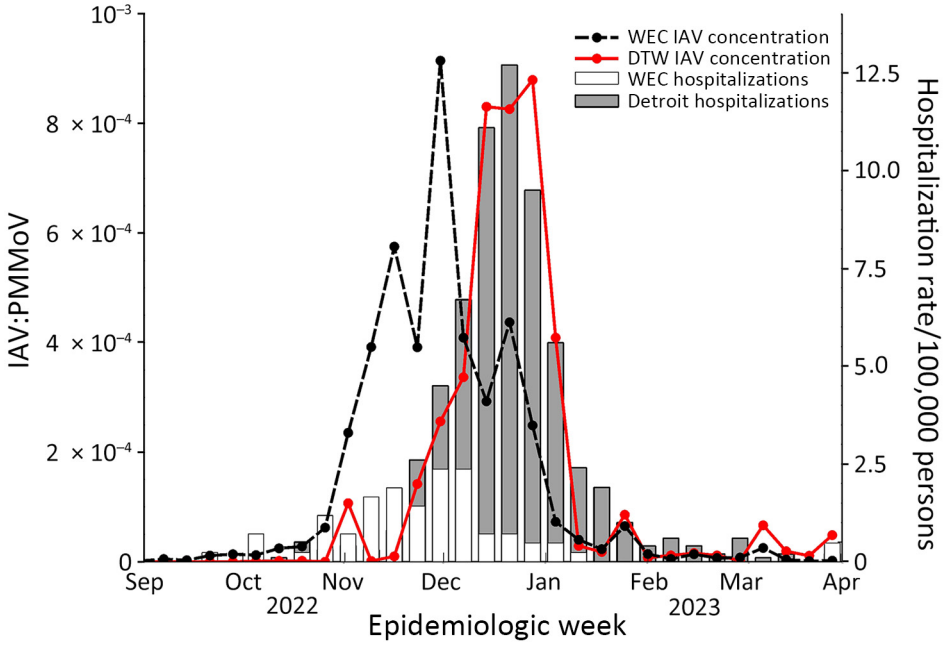

Figure. Influenza-associated hospitalization rates and aggregate population-weighted wastewater concentrations for influenza A virus, by epidemiologic week, in Windsor-Essex, Ontario, Canada, and Detroit, Michigan, USA, September 2022–March 2023. The population-weighted PMMoV normalized IAV concentration (lines) is superimposed over the rate of influenza-related hospitalizations (bars). DTW, Detroit wastewater; IAV, influenza A virus; PMMoV, pepper mild mottle virus; WEC, Windsor-Essex County wastewater.

Table 1. Temporal shift at which peak synchrony was found between concentrations of influenza A in wastewater and influenza-associated hospitalizations for Windsor-Essex, Ontario, Canada (September 2022–March 2023), and Detroit, Michigan, USA (October 2022–March 2023)*

Associations†	Peak synchrony, wk	Spearman ρ
WEC M1:PMMoV and influenza-associated hospitalizations	1	0.797
WEC M1 and influenza-associated hospitalization	1	0.841
DTW M1:PMMoV and influenza-associated hospitalizations	0	0.708
DTW M1 and influenza-associated hospitalizations	0	0.769
WEC M1:PMMoV and DTW M1:PMMoV	−3	0.642
WEC M1 and DTW M1	−3	0.695

*Peak synchrony was also found between Windsor-Essex and Detroit influenza A wastewater signals during September 2022–March 2023. Wastewater signals were shifted, and clinical metrics remained stationary. Positive values indicate a lagging wastewater signal and negative values indicate a leading wastewater signal. DTW, Detroit wastewater; M1, matrix 1 gene: PMMoV, pepper mottle mild virus; WEC, Windor-Essex County wastewater.
†DTW M1, aggregate concentration of influenza A M1 gene (genome copies/mL) in DTW; DTW M1:PMMoV, concentration of influenza A M1 gene in DTW normalized to PMMoV (unitless); WEC M1, aggregate concentration of influenza A M1 gene in WEC (gc/L); WEC M1:PMMoV, concentration of influenza A M1 gene in WEC normalized to PMMoV concentration (unitless).

either community when analyzed on an epidemiologic week basis; wastewater signal either lagged or was synchronous with hospitalization data. Observation of synchronous or delayed wastewater signal is not without precedent. Recent surveillance efforts have noted lagging wastewater signals (*29*). Other studies have cited the predictive ability of WS in the context of influenza monitoring (*13*,*14*,*30*). In our study, application of blockwise averaging to produce average concentrations of IAV RNA by epidemiologic week could have masked lead time within the data.

Viral load in influenza patients may peak 1–2 days after symptom onset on the basis of nose and throat swab testing results, and shedding may last 6–7 days (*31*). A meta-analysis of challenge studies examining respiratory tract shedding found shedding lasts an average of 4.8 days, and peak shedding rates occur 2 days after exposure (*32*). A clinical study reported that 41% of IAV-positive patients produced detectable levels of IAV RNA in their feces (*11*). Another study of hospitalized patients found that 47% of people infected with IAV shed IAV RNA in their feces (*33*). Because only some people shed IAV RNA in feces, incubation periods are short, and viral loads rapidly peak, WS loses its ability to predict influenza-associated hospitalizations when the temporal granularity of incidence data is limited. However, producing meaningful data through clinical testing takes longer than results from WS. Case data obtained through laboratory-based virology are released weeks after testing occurs and are often subject to revision because results may reflect data compiled from multiple laboratories. WS can provide more timely measures of incidence because sample processing, RNA quantification, data analysis, and reporting are often completed the same day as sample collection in Windsor-Essex. WS can be considered de facto lead-time because data may be disseminated to public health officials well in advance of case data.

The utility of WS is not restricted to predictive ability. WS is an independent and sensitive measure of disease prevalence (*34*), enabling it to be used as an additional metric for trend comparison across jurisdictional boundaries, and it may be helpful when testing conventions and public health policies differ. Unlike WS, influenza cases and hospitalizations likely represent only the most severe cases of influenza in which people sought medical testing and treatment, and they do not necessarily represent population-wide trends. WS has the potential to aid in accurately tracking infection dynamics when testing capacity is limited or few patients seek medical care.

In the case of Windsor-Essex and Detroit, the cross-border movement of persons and goods is vital to the region because of strong economy integration (*35*). Many people, such as healthcare and automotive workers, commute across the border daily to work in Michigan while living in Ontario (*16*). Almost 18,000 people crossed into Windsor-Essex from Detroit daily over the course of our study, which suggests

Table 2. Unshifted correlations between influenza-associated hospitalizations and the aggregate population-weighted wastewater concentrations for influenza A virus in Windsor-Essex, Ontario, Canada, September 2022–March 2023*

Associations†	Statistical test results			
	Kendall τ	Spearman ρ	2-tailed 95% CI‡	2-tailed p value
WEC M1 and influenza-associated hospitalization	0.650		0.482–0.772	<0.001
WEC M1:PMMoV and influenza-associated hospitalizations	0.630		0.456–0.758	<0.001
WEC M1 and influenza-associated hospitalization		0.785	0.589–0. 893	<0.001
WEC M1:PMMoV and influenza-associated hospitalizations		0.754	0.538–0.877	<0.001

*M1, matrix 1 gene: PMMoV, pepper mottle mild virus; WEC, Windor-Essex County wastewater.
†WEC M1, aggregate concentration of influenza A M1 gene in WEC (gc/L); WEC M1:PMMoV, concentration of influenza A M1 gene in WEC normalized to PMMoV concentration (unitless).
‡Estimation is based on Fisher r-to-z transformation; estimation of SE is based on the formula proposed by Fieller, Hartley, and Pearson (*27*).

Table 3. Unshifted correlations between influenza-associated hospitalizations in Michigan, USA, and the aggregate population-weighted wastewater concentrations for influenza A virus in Detroit, MI, USA from October 2022–March 23*

Associations†	Statistical test results		2-tailed 95% CI‡		2-tailed p value
	Kendall τ	Spearman ρ			
DTW M1 and influenza-associated hospitalizations	0.616		0.415	0.759	<0.001
DTW M1:PMMoV and influenza-associated hospitalizations	0.559		0.341	0720	<0.001
DTW M1 and influenza-associated hospitalizations		0.769	0.535	0.893	<0.001
DTW M1:PMMoV and influenza-associated hospitalizations		0.708	0. 433	0.863	<0.001

*DTW, Detroit wastewater; M1, matrix 1 gene: PMMoV, pepper mottle mild virus.
†DTW M1, aggregate concentration of influenza A M1 gene (genome copies/mL) in DTW; DTW M1:PMMoV, concentration of influenza A M1 gene in DTW normalized to PMMoV (unitless).
‡Estimation is based on Fisher r-to-z transformation; estimation of SE is based on the formula proposed by Fieller, Hartley, and Pearson (*27*).

the communities could have concurrent influenza seasons (Appendix Figure 1). Contrary to this expectation, we observed the peak and onset of the 2022–23 IAV wastewater signal in Detroit was delayed by ≈3 weeks when compared with Windsor-Essex. An explanation for this discrepancy could be the lingering effect of travel restrictions implemented during the COVID-19 pandemic, which limited travel between these interconnected cities (Appendix Figure 1). There was no restriction on trade or the commutes of essential workers, and testing requirements for cross-border travel ended in April 2022. The remaining COVID-19 related travel restrictions were lifted at the start of October 2022, before the onset of the influenza season. Despite the removal of restrictions, the number of people crossing into Windsor-Essex each day during the second half of 2022 was ≈25% less than the number of people crossing prior to the COVID-19 pandemic (17,867 vs. 24,260) (Appendix Figure 2). The residual effect of border restrictions, evidenced by the suppressed cross-border traffic in the leadup to the 2022–23 respiratory season, shows that border restrictions could have played a role in the observed discrepancies between Windsor-Essex and Detroit.

Another potential cause of the timing difference in the influenza seasons between Detroit and Windsor-Essex could be pandemic mitigation strategies, such as mask mandates and social distancing guidance. Ontario was slower to implement a mask mandate but kept the mandate in place much longer than Michigan did. Michigan lifted all masking requirements on June 22, 2021, whereas Ontario ended its mask mandate 272 days later, on March 21, 2022 (*36*,*37*). Michigan ending the mask mandate early could have enabled the circulation of influenza in Detroit before the 2022–23 respiratory season, increasing levels of natural immunity in Michigan. However, clinical data and wastewater surveillance in Windsor-Essex show that influenza was circulating in Windsor-Essex in spring 2022 (Appendix Figure 3).

Differences in influenza immunization campaigns might also explain the differences in influenza season onset between Detroit and Windsor-Essex. Influenza vaccines could have played a role in determining the effective reproduction number for IAV in the 2022–23 season. Preliminary research showed the vaccine effectiveness (VE) in Canada against IAV subtype H3N2 was 54% for people <65 years of age (*17*). H3N2 was the dominant IAV subtype, representing ≈95% of cases (*17*), in contrast with the limited sequencing results of a selection of amplicons (Appendix Figure 4). Similar estimates of VE for this cohort were produced for Wisconsin (60%) (*38*) and across the United States (51%) (*39*). Michigan and Ontario use similar vaccines, with a focus on administering quadrivalent-inactivated influenza vaccines to the population (*40*,*41*). Although inoculation with some vaccine types, such as live attenuated vaccines, is associated with viral shedding, it is unlikely to contribute to wastewater signals (*42*). Because VE and vaccine type were similar between Michigan and Ontario, the differentiating factor could be inoculation timing. Influenza vaccine distribution in Michigan typically begins earlier than Ontario, with inoculations happening as early as July. By November 2022, a total of 2,632,430 Michigan residents were vaccinated (≈25% of the population) (*43*). Inoculation efforts in Ontario began later, and vaccines were not made available to all residents until November (*44*). Mass influenza inoculation efforts in Ontario began after IAV RNA concentration started increasing in the wastewater, signaling the start of the influenza season. Vaccination campaigns were already well under way in Michigan when the IAV RNA concentration began to increase in wastewater. We speculate that people from Ontario were less likely to have vaccine-induced immunity than those from Michigan early in the season, potentially contributing to the earlier peak in Windsor-Essex wastewater IAV signal. However, it is unclear if the timing of vaccine campaigns contributed to the observed difference between the Michigan and Ontario influenza seasons. Additional factors, including socio-economic status (*45*), access to healthcare, racial demographics (*46*), population age structure (*47*), and virus–virus interactions (*48*) could have contributed to the differences. Population-level administration schedules for

seasonal influenza vaccines merit further investigation; those schedules help determine when herd immunity is reached and if herd immunity is reached before the spread of illness within a community.

The first limitation of our study is that WRRF does not serve the Michigan counties where FluSurv-NET–participating hospitals are located. However, both the hospitalization data garnered from FluSurv-Net and wastewater data can be considered a proxy for statewide incidence. All influenza-associated hospitalizations were included in this dataset, for both Michigan and Windsor-Essex, even though the WS focused only on IAV. Our analysis could have been affected by focus on IAV, despite its dominance in the 2022–23 influenza season (*17*). Not all hospitalizations recorded in the Windsor-Essex data were laboratory confirmed cases of influenza. The temporal resolution of sample collection at the WRRF was limited, and weekly sampling might have failed to capture variability in the wastewater signal. Finally, the wastewater treatment plants monitored in both Windsor-Essex and Detroit, although serving representative populations, do not encompass all the residents and could have failed to capture variability in IAV wastewater signal.

In conclusion, our study demonstrates how wastewater surveillance can shed light on regional differences that may have otherwise gone unnoticed, or remain unvalidated, because of the inherent limitations of traditional metrics to capture population-wide trends. Future studies investigating influenza vaccine administration schedules should incorporate WS as an independent metric of disease incidence. WS can potentially provide more timely measures of incidence, rather than waiting for the release of laboratory testing. The utility of WS as a predictive metric, and as a metric for trend comparison across jurisdictional boundaries with different approaches to vaccination and collecting disease incidence metrics, demonstrates its usefulness when testing conventions and public health policies differ.

Acknowledgments

We thank the employees and management of the following wastewater treatment facilities for their collaboration: Wastewater Resource Recovery Facility, Great Lakes Water Authority; Pollution Control, City of Windsor.

Funding was provided by the Ontario Ministry of Environment, Conservation, and Parks, the Government of Canada's New Frontiers in Research Fund (grant no. NFRFR-2022-00416), the Canada Biomedical Research Fund (grant no. CBRF2-2023-00008), and Ontario Genomics.

About the Author

Mr. Corchis-Scott is a PhD candidate in environmental science at the Great Lakes Institute for Environmental Research at the University of Windsor. His research interests include wastewater-based surveillance of respiratory pathogens, antimicrobial resistance genes, conservation genetics, and a One Health approach to advancing human health.

References

1. Fauci AS, Folkers GK. Pandemic preparedness and response: lessons from COVID-19. J Infect Dis. 2023;228:422–5. https://doi.org/10.1093/infdis/jiad095
2. Havasi A, Visan S, Cainap C, Cainap SS, Mihaila AA, Pop LA. Influenza A, influenza B, and SARS-CoV-2 similarities and differences—a focus on diagnosis. Front Microbiol. 2022;13:908525. https://doi.org/10.3389/fmicb.2022.908525
3. Yuan P, Aruffo E, Tan Y, Yang L, Ogden NH, Fazil A, et al. Projections of the transmission of the omicron variant for Toronto, Ontario, and Canada using surveillance data following recent changes in testing policies. Infect Dis Model. 2022;7:83–93. https://doi.org/10.1016/j.idm.2022.03.004
4. Koplan JP, Butler-Jones D, Tsang T, Yu W. Public health lessons from severe acute respiratory syndrome a decade later. Emerg Infect Dis. 2013;19:861–3. https://doi.org/10.3201/eid1906.121426
5. Wright J, Driver EM, Bowes DA, Johnston B, Halden RU. Comparison of high-frequency in-pipe SARS-CoV-2 wastewater-based surveillance to concurrent COVID-19 random clinical testing on a public U.S. university campus. Sci Total Environ. 2022;820:152877. https://doi.org/10.1016/j.scitotenv.2021.152877
6. Yoo BK, Iwamoto R, Chung U, Sasaki T, Kitajima M. Economic evaluation of wastewater surveillance combined with clinical COVID-19 screening tests, Japan. Emerg Infect Dis. 2023;29:1608–17. https://doi.org/10.3201/eid2908.221775
7. D'Aoust PM, Graber TE, Mercier E, Montpetit D, Alexandrov I, Neault N, et al. Catching a resurgence: increase in SARS-CoV-2 viral RNA identified in wastewater 48 h before COVID-19 clinical tests and 96 h before hospitalizations. Sci Total Environ. 2021;770:145319. https://doi.org/10.1016/j.scitotenv.2021.145319
8. Ahmed W, Tscharke B, Bertsch PM, Bibby K, Bivins A, Choi P, et al. SARS-CoV-2 RNA monitoring in wastewater as a potential early warning system for COVID-19 transmission in the community: a temporal case study. Sci Total Environ. 2021;761:144216. https://doi.org/10.1016/j.scitotenv.2020.144216
9. Diamond MB, Keshaviah A, Bento AI, Conroy-Ben O, Driver EM, Ensor KB, et al. Wastewater surveillance of pathogens can inform public health responses. Nat Med. 2022;28:1992–5. https://doi.org/10.1038/s41591-022-01940-x
10. Rolfes MA, Foppa IM, Garg S, Flannery B, Brammer L, Singleton JA, et al. Annual estimates of the burden of seasonal influenza in the United States: a tool for strengthening influenza surveillance and preparedness. Influenza Other Respir Viruses. 2018;12:132–7. https://doi.org/10.1111/irv.12486
11. Al Khatib HA, Coyle PV, Al Maslamani MA, Al Thani AA, Pathan SA, Yassine HM. Molecular and biological characterization of influenza A viruses isolated from human

fecal samples. Infect Genet Evol. 2021;93:104972. https://doi.org/10.1016/j.meegid.2021.104972
12. Toribio-Avedillo D, Gómez-Gómez C, Sala-Comorera L, Rodríguez-Rubio L, Carcereny A, García-Pedemonte D, et al. Monitoring influenza and respiratory syncytial virus in wastewater. Beyond COVID-19. Sci Total Environ. 2023; 892:164495. https://doi.org/10.1016/j.scitotenv.2023.164495
13. Mercier E, D'Aoust PM, Thakali O, Hegazy N, Jia JJ, Zhang Z, et al. Municipal and neighbourhood level wastewater surveillance and subtyping of an influenza virus outbreak. Sci Rep. 2022;12:15777. https://doi.org/10.1038/s41598-022-20076-z
14. Ahmed W, Bivins A, Stephens M, Metcalfe S, Smith WJM, Sirikanchana K, et al. Occurrence of multiple respiratory viruses in wastewater in Queensland, Australia: potential for community disease surveillance. Sci Total Environ. 2023; 864:161023. https://doi.org/10.1016/j.scitotenv.2022.161023
15. Maoh H, Dimatulac T, Khan S, Litwin M. Studying border crossing choice behavior of trucks moving between Ontario, Canada and the United States. J Transp Geogr. 2021;91:102992. https://doi.org/10.1016/j.jtrangeo.2021.102992
16. Dunphy S. Cross-border labour mobility in the Windsor-Detroit region: the case of nurses. The Estey Centre Journal of International Law and Trade Policy. 2015;16:14–38.
17. Skowronski DM, Chuang ES, Sabaiduc S, Kaweski SE, Kim S, Dickinson JA, et al. Vaccine effectiveness estimates from an early-season influenza A(H3N2) epidemic, including unique genetic diversity with reassortment, Canada, 2022/23. Euro Surveill. 2023;28:2300043. https://doi.org/10.2807/1560-7917.ES.2023.28.5.2300043
18. Kim S, Chuang ES, Sabaiduc S, Olsha R, Kaweski SE, Zelyas N, et al. Influenza vaccine effectiveness against A(H3N2) during the delayed 2021/22 epidemic in Canada. Euro Surveill. 2022;27:2200720. https://doi.org/10.2807/1560-7917.ES.2022.27.38.2200720
19. Centers for Disease Control and Prevention. Preliminary flu burden estimates, 2021–22 season. 2023 [cited 2024 Apr 11]. https://www.cdc.gov/flu/about/burden/2021-2022.htm
20. Michigan Department of Health & Human Services. Past Michigan flu focus reports [cited 2023 Sep 28]. https://www.michigan.gov/flu/surveillance/past-michigan-flu-focus-surveillance-reports
21. Zhao L, Geng Q, Corchis-Scott R, McKay RM, Norton J, Xagoraraki I. Targeting a free viral fraction enhances the early alert potential of wastewater surveillance for SARS-CoV-2: a methods comparison spanning the transition between delta and omicron variants in a large urban center. Front Public Health. 2023;11:1140441. https://doi.org/10.3389/fpubh.2023.1140441
22. CDM Smith. Great Lakes Water Authority wastewater master plan. 2020 Jun [cited 2024 Apr 23]. https://www.glwater.org/wp-content/uploads/2020/12/Full_WWMP_Report_Final_June-2020.pdf
23. Centers for Disease Control and Prevention. CDC's influenza SARS-CoV-2 multiplex assay. 2020 [cited 2023 Sep 20]. https://www.cdc.gov/coronavirus/2019-ncov/lab/multiplex.html
24. Rosario K, Symonds EM, Sinigalliano C, Stewart J, Breitbart M. Pepper mild mottle virus as an indicator of fecal pollution. Appl Environ Microbiol. 2009;75:7261–7. https://doi.org/10.1128/AEM.00410-09
25. Centers for Disease Control and Prevention. Influenza Hospitalization Surveillance Network. 2024 [cited 2024 Apr 11]. https://www.cdc.gov/flu/weekly/influenza-hospitalization-surveillance.htm
26. Rauch W, Schenk H, Insam H, Markt R, Kreuzinger N. Data modelling recipes for SARS-CoV-2 wastewater-based epidemiology. Environ Res. 2022;214:113809. https://doi.org/10.1016/j.envres.2022.113809
27. Fieller EC, Hartley HO, Pearson ES. Tests for rank correlation coefficients. I. Biometrika. 1957;44:470–81. https://doi.org/10.1093/biomet/44.3-4.470
28. DeJonge PM, Adams C, Pray I, Schussman MK, Fahney RB, Shafer M, et al. Wastewater surveillance data as a complement to emergency department visit data for tracking incidence of influenza A and respiratory syncytial virus — Wisconsin, August 2022–March 2023. MMWR Morb Mortal Wkly Rep. 2023;72:1005–9. https://doi.org/10.15585/mmwr.mm7237a2
29. Faherty EAG, Yuce D, Korban C, Bemis K, Kowalski R, Gretsch S, et al. Correlation of wastewater surveillance data with traditional influenza surveillance measures in Cook County, Illinois, October 2022-April 2023. Sci Total Environ. 2024;912:169551. https://doi.org/10.1016/j.scitotenv.2023.169551
30. Schoen ME, Bidwell AL, Wolfe MK, Boehm AB. United States influenza 2022–2023 season characteristics as inferred from wastewater solids, influenza hospitalization, and syndromic data. Environ Sci Technol. 2023;57:20542–50. https://doi.org/10.1021/acs.est.3c07526
31 Ip DKM, Lau LLH, Chan KH, Fang VJ, Leung GM, Peiris MJS, et al. The dynamic relationship between clinical symptomatology and viral shedding in naturally acquired seasonal and pandemic influenza virus infections. Clin Infect Dis. 2016;62:431–7.
32. Carrat F, Vergu E, Ferguson NM, Lemaitre M, Cauchemez S, Leach S, et al. Time lines of infection and disease in human influenza: a review of volunteer challenge studies. Am J Epidemiol. 2008;167:775–85. https://doi.org/10.1093/aje/kwm375
33. Chan MCW, Lee N, Chan PKS, To KF, Wong RYK, Ho WS, et al. Seasonal influenza A virus in feces of hospitalized adults. Emerg Infect Dis. 2011;17:2038–42. https://doi.org/10.3201/eid1711.110205
34. Mattei M, Pintó RM, Guix S, Bosch A, Arenas A. Analysis of SARS-CoV-2 in wastewater for prevalence estimation and investigating clinical diagnostic test biases. Water Res. 2023;242:120223. https://doi.org/10.1016/j.watres.2023.120223
35. Brunet-Jailly E. Cross-border cooperation: a global overview. Alternatives (Boulder). 2022;47:3–17. https://doi.org/10.1177/03043754211073463
36. Jabakhanji S, Knope J. Ontario to drop most mask mandates on March 21, remaining pandemic rules to lift by end of April. 2022 [cited 2023 Sep 28]. https://www.cbc.ca/news/canada/toronto/covid19-ontario-march-9-mask-mandates-1.6378148
37. Boucher D. Michigan ends most COVID-19 restrictions today: what it means for you [cited 2023 Nov 23]. https://www.freep.com/story/news/local/michigan/2021/06/22/covid-updates-michigan-restrictions-mask-mandate/7774556002/
38. McLean HQ, Petrie JG, Hanson KE, Meece JK, Rolfes MA, Sylvester GC, et al. Interim estimates of 2022-23 seasonal influenza vaccine effectiveness — Wisconsin, October 2022–February 2023. MMWR Morb Mortal Wkly Rep. 2023;72:201–5 https://doi.org/10.15585/mmwr.mm7208a1
39. Centers for Disease Control and Prevention. Preliminary flu vaccine effectiveness (VE) data for 2022–2023. 2023 [cited 2023 Oct 26]. https://www.cdc.gov/flu/vaccines-work/2022-2023.html

40. Public Health Sudbury & Districts. Influenza vaccine availability for the 2022/2023 season [cited 2023 Sep 28]. https://www.phsd.ca/professionals/health-professionals/advisory-alerts-health-care-professionals/influenza-vaccine-availability-for-the-2022-2023-season
41. Michigan Department of Health and Human Services, Division of Immunization. Seasonal influenza vaccines 2023–2024. 2023. [cited 2023 Sep 28]. https://www.michigan.gov/flu/-/media/Project/Websites/flu/Flu-Presentation-Chart-23-24_FINAL.pdf
42. Armas F, Chandra F, Lee WL, Gu X, Chen H, Xiao A, et al. Contextualizing wastewater-based surveillance in the COVID-19 vaccination era. Environ Int. 2023;171:107718. https://doi.org/10.1016/j.envint.2022.107718
43. Michigan Department of Health & Human Services. Flu dashboard [cited 2023 Sep 28]. https://www.michigan.gov/flu/flu-dashboard
44. Moore KM. Ontario's universal influenza immunization program (UIIP)–2022/2023. 2022 [cited 2023 Sep 28]. https://www.wechu.org/sites/default/files/pdf/2022-23_UIIP_CMOH_letter_to_HCPs_EN.pdf
45. Mamelund SE, Shelley-Egan C, Rogeberg O. The association between socioeconomic status and pandemic influenza: systematic review and meta-analysis. PLoS One. 2021;16:e0244346. https://doi.org/10.1371/journal.pone.0244346
46. Kurupati R, Kossenkov A, Haut L, Kannan S, Xiang Z, Li Y, et al. Race-related differences in antibody responses to the inactivated influenza vaccine are linked to distinct pre-vaccination gene expression profiles in blood. Oncotarget. 2016;7:62898–911. https://doi.org/10.18632/oncotarget.11704
47. Jayasundara K, Soobiah C, Thommes E, Tricco AC, Chit A. Natural attack rate of influenza in unvaccinated children and adults: a meta-regression analysis. BMC Infect Dis. 2014;14:670. https://doi.org/10.1186/s12879-014-0670-5
48. Pinky L, Dobrovolny HM. Epidemiological consequences of viral interference: a mathematical modeling study of two interacting viruses. Front Microbiol. 2022;13:830423. https://doi.org/10.3389/fmicb.2022.830423

Address for correspondence: Ryland Corchis-Scott, Great Lakes Institute for Environmental Research, University of Windsor, 401 Sunset Ave, Windsor, ON N9B 3P4, Canada; email: corchisr@uwindsor.ca

etymologia revisited

Malaria
[mə-lar'e-ə]

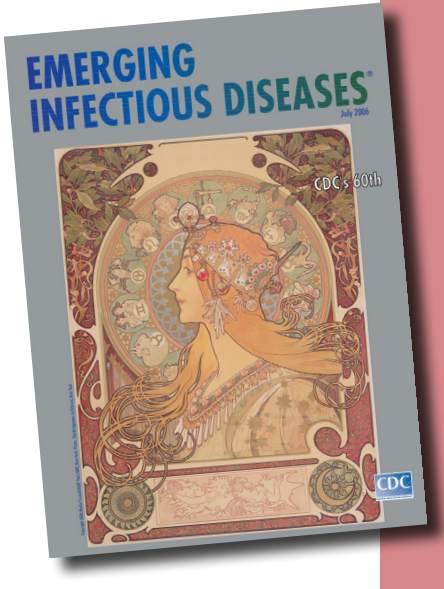

Originally published in July 2006

Malaria, "bad air" in Italian, was blamed for the deaths of >1,000 workers digging the Erie Canal in 1819. Work on the canal continued in winter, when the swamp was frozen over (and, although the vector was not known at the time, mosquitoes were dormant). Malaria, caused by parasites of the genus *Plasmodium* and usually transmitted by the bite of infected *Anopheles* mosquitoes, is endemic in many warm regions. Charles Louis Alphonse Laveran discovered the protozoan cause of malaria in 1880. The Office of Malaria Control in War Areas, which was established in 1942 to control malaria and other vectorborne diseases in the southern United States, evolved into what is today the Centers for Disease Control and Prevention.

Source:
Dorland's illustrated medical dictionary. 30th ed. Philadelphia: Saunders; 2003; cdc.gov; and wikipedia.org

https://wwwnc.cdc.gov/eid/article/12/7/ET-1207_article

Article DOI: https://doi.org/10.3201/eid3008.240225

Wastewater Surveillance to Confirm Differences in Influenza A Infection between Michigan, USA, and Ontario, Canada, September 2022–March 2023

Appendix

Appendix Methods

Sample Collection

Untreated wastewater samples were collected five times per week from two different wastewater treatment plants located in Windsor-Essex between September 1st, 2022, and March 31, 2023. Sample collection spanned a 31-week period. The Lou Romano Water Reclamation Plant (LRWRP) serves ≈180,000 individuals and is the largest treatment facility in Windsor-Essex. The Little River Pollution Control Plant (LRPCP) serves 90,000 persons and together with LRWRP these plants service the majority of Windsor-Essex's urban center. Concurrently, samples were collected from the Water Resource Recovery Facility (WRRF) operated by the Great Lakes Water Authority (GLWA) located in Detroit, MI at a frequency of one sample per week. The WRRF facility serves the majority of the greater metropolitan Detroit area and treats the waste of ≈3 million individuals, which equates to roughly a third of the population of the state of Michigan. The plant treats the combined stormwater, industrial, residential, and commercial waste that arrive through three major interceptors. These are the Detroit River Interceptor, the North Interceptor-East Arm and the Oakwood-Northwest-Wayne County Interceptor which serve a large region of southeast Michigan including the City of Detroit. All samples collected in both Windsor-Essex and Detroit were 1L 24-hour composite samples composed of aliquots of wastewater removed from the influent stream regular intervals. Following collection, samples were transported on ice to the laboratory for immediate concentration and analysis.

Sample Processing

Composite samples of raw wastewater were concentrated by filtering 50–120 mL through 0.22 µm Sterivex PES cartridge filters (MilliporeSigma, Burlington, MA, USA) using a 60 mL syringe fitted into a caulking gun. Immediately following filtration, the filters were sealed and flash-frozen through immersion in liquid nitrogen. Subsequently, filters were subjected to downstream processes including RNA extraction and RT-qPCR.

Following filtration and flash freezing, filters were thawed, and the filter membrane was cut from the Sterivex cartridge using a sterile scalpel and forceps. Total nucleic acid was extracted from the filter membranes using either the AllPrep PowerViral DNA/RNA kit (Qiagen, Germantown, MD, USA) modified by addition of 5% 2-mercaptoethanol (v/v) or the RNeasy PowerMicrobiome Kit (Qiagen, Germantown, MD, USA), again modified by addition of 5% 2-mercaptoethanol (v/v). Samples were not treated with DNase upon extraction and RNA was eluted in 50µL of RNase free water.

RT-qPCR

An RT-qPCR assay was used to measure the concentration of influenza A virus (IAV) in wastewater samples. The assay targeted RNA that codes for the matrix protein 1 (M1-gene) of IAV using primers and probes developed by the U.S. CDC (*1*). Primers and probes were supplied by Integrated DNA Technologies (Coralville, IA, USA) and primer and probe sequences can be found in Supplementary Table 1.

Appendix Table 1. Primer/probe sequences for RT-qPCR of IAV M1 gene

IAV Assay	Sequence
Forward Primer	5′-CAAGACCAATCYTGTCACCTCTGAC-3′
Reverse Primer	5′-GCATTYTGGACAAAVCGTCTACG-3′
Probe	5′-/FAM/TGCAGTCCT/ZEN/CGCTCACTGGGCACG/3IABkFQ/-3′

Reactions contained 4µL of RNA template mixed with 10µL of Luna Universal Probe One-Step Reaction Mix (2X), 1µL Luna WarmStart® RT Enzyme Mix (20X) (Luna® One-Step RT-qPCR Kit, Massachusetts, USA), forward primer (final concentration of 500nM), reverse primer (final concentration of 500nM), and probe (final concentration of 250nM) in a final reaction volume of 20µL. RT was performed at 55°C for 10 min, followed by polymerase activation at 95°C for 1 min, and 45 cycles of denaturation, annealing/extension at 95°C for 10 sec, then 55°C for 45 sec, respectively. No template controls yielded no amplification, and the limit of detection for the assay was determined at 4 gene copies of IAV per reaction containing

4µL of template RNA, corresponding to a greater than 95% probability of detection. LOD was determined through analysis of 20 replicate 8-point standard curves. Twist Synthetic Influenza H3N2 RNA control (Twist Bioscience, San Francisco, CA) was used to create an 8-point standard curve to quantify gene targets. RT-qPCR assays were also performed to evaluate the levels of Pepper Mild Mottled Virus (PMMoV) within the wastewater. PMMoV is a widely accepted indicator of the presence of human fecal matter (*2–4*). For quantification of PMMoV, reactions contained 2.5µL of RNA template mixed with 10µL of Luna Universal Probe One-Step Reaction Mix (2X), 1µL Luna WarmStart® RT Enzyme Mix (20X) (Luna® One-Step RT-qPCR Kit, Massachusetts, USA), 3.5µL of water and the remaining 3µL consisted of forward primer, reverse primer, and probe each with a final concentration of 200nM. Primers and probes for the amplification of PMMoV were previously described (*5*). Reverse transcription was performed for 10 minutes at 55°C, this was followed by an enzyme activation step at 95°C for 1 minute and 40 cycles of denaturation and annealing/extension at 95°C for 10 seconds and 55°C for 30 seconds respectively. No template controls were included with each plate of RT-qPCR run and whole process controls were included with each extraction. The 7-point standard curve for the quantification of PMMoV was generated through serial dilution of a custom gBlock (Integrated DNA Technologies, Coralville, IA, USA) and was run with each plate of samples. No amplification was observed either process controls (extraction blanks) or in no template controls. Reaction inhibition was assessed using VetMAX XENO Internal Positive Control RNA (Applied Biosystems Corp., Waltham, MA, USA). VetMax template was spiked into water (which was used as a reference), undiluted DNA/RNA extracts, DNA/RNA extracts diluted 1:5, and DNA/RNA extracts diluted 1:10. Recovery was compared between conditions, and it was determined that inhibition could be addressed through dilution. Due to repeated incidence of inhibition with wastewater samples processed by filtration, template was diluted 1:5 or 1:10 in all reactions. Technical triplicates were run for detection of gene targets. Thermal cycling was performed using a MA6000 qPCR thermocycler (Sansure Biotech, Changsha, China).

Amplicon Sequencing

To validate the identity of the amplicon obtained from M1 gene of IAV, RTq-PCR products obtained from IAV-positive wastewater samples were sequenced. First, the PCR products were cleaned up by adding 1 volume of NEBNext® Sample Purification Beads (NEB).

DNA was eluted in 15 µL Nuclease-free water and quantified using Denovix DS-11 Spectrophotometer.

Second, the end-prep reaction was performed employing 250–300 ng of DNA mixed with 1.75 µL UltraII End Prep Buffer, 0.75 µL UltraII End Prep Enzyme and water to a final volume of 15 µL. The reaction was incubated at 20°C for 10 minutes and 65°C for 10 minutes, holding at 4°C. Barcoding of samples was carried out combining 3 µL of end-prepped sample, 2.5 µL Native Barcode (ONT, native barcoding EXP-NBD104), 10 µL Blunt/TA Ligase Master Mix and 4.5 µL nuclease-free water. Samples were pooled after barcoding and then analyzed in a single sequencing run with separated reads obtained from each of the amplicons. Ligation reaction was incubated at 22°C for 20 minutes and 65°C for 10 minutes, followed by a hold on ice for at least 1 minute. Cleaning up of the ligated sample was performed by adding 0.4 volume NEBNext® Sample Purification Beads and eluting with 12 µL of nuclease-free water. The Oxford Nanopore sequencing adaptor ligation was performed employing 200 ng of barcoded DNA in 30 µL, mixed with 5 µL Adaptor Mix II, 10 µL 5X NEBNext Quick Ligation Reaction Buffer (NEB) and 5 µL Quick T4 DNA Ligase (NEB). The incubation was carried out at 25°C for 30 minutes. Sample was cleaned up by adding 1 volume of NEBNext® Sample Purification Beads, eluted in 12 µL of Elution Buffer and quantified. Twenty ng of the library was loaded onto a SpotOn Flow Cell (R9.4 flow cell). Data was collected along 16 hours of sequencing with MinION.The FastQ files containing the sequenced reads were uploaded in Epi2me desktop application (Oxford Nanopore Technologies). Reads were analyzed employing the WIMP (*What's In My Pot*) workflow (v2023.06.13–1865548) setting filters for reads length between 100 bp to 250 bp. WIMP initially filters FASTQ files with a mean q-score below a minimum threshold (defaults to 7). For reads above the quality threshold, the Centrifuge classification engine is executed to assign each read to a taxon in the NCBI taxonomy. Taxonomical assignment is done based on the scores calculated by the microbial classification engine called Centrifuge using default settings where the minimum length of partial hits is set to 25 (min_hit_len) and the minimum summed length of partial hits is set to 0 (*6*). Manual calculation of the identity % for the taxonomical assignments was not completed. The Centrifuge classification results are then filtered and aggregated to calculate and report counts of reads at the species rank. For reads without a reliable assignment at the species rank, higher ranks of the

taxonomy tree are used for the assignment. Supplementary Figure 4 shows a taxonomic tree of IAV sequences detected through Nanopore sequencing of the amplicons.

Additionally, several filtered sequences were randomly selected and manually uploaded to Basic Local Alignment Search Tool (BLAST) to confirm the identity of the M1 gene portion amplified by RT-qPCR. Raw sequencing data was uploaded to the National Center for Biotechnology Information (NCBI) Sequence Read Archive (SRA). Raw sequence data have the following accessions: SAMN39936024, SAMN39936025, SAMN39936026, SAMN39936027, and SAMN39936028.

References

1. Centers for Disease Control and Prevention. CDC's influenza SARS-CoV-2 multiplex assay. 2020 [cited 2023 Sep 20]. https://www.cdc.gov/coronavirus/2019-ncov/lab/multiplex.html

2. Rosario K, Symonds EM, Sinigalliano C, Stewart J, Breitbart M. Pepper mild mottle virus as an indicator of fecal pollution. Appl Environ Microbiol. 2009;75:7261–7. PubMed https://doi.org/10.1128/AEM.00410-09

3. Kitajima M, Sassi HP, Torrey JR. Pepper mild mottle virus as a water quality indicator. NPJ Clean Water. 2018;1:1–9. https://doi.org/10.1038/s41545-018-0019-5

4. Zhang T, Breitbart M, Lee WH, Run JQ, Wei CL, Soh SWL, et al. RNA viral community in human feces: prevalence of plant pathogenic viruses. PLoS Biol. 2006;4:e3. PubMed https://doi.org/10.1371/journal.pbio.0040003

5. Haramoto E, Kitajima M, Kishida N, Konno Y, Katayama H, Asami M, et al. Occurrence of pepper mild mottle virus in drinking water sources in Japan. Appl Environ Microbiol. 2013;79:7413–8. PubMed https://doi.org/10.1128/AEM.02354-13

6. Kim D, Song L, Breitwieser FP, Salzberg SL. Centrifuge: rapid and sensitive classification of metagenomic sequences. Genome Res. 2016;26:1721–9. PubMed https://doi.org/10.1101/gr.210641.116

7. Canada Border Services Agency. Traveller volumes by port of entry and month. 2024 [cited 2024 Jan 30]. https://open.canada.ca/data/dataset/1b1c2b92-b388-47d9-87d4-01aee8d3c3e4

8. The Windsor-Essex County Health Unit. Weekly Influenza Bulletin Data Dashboard. [cited 2023 Sep 28]. https://www.wechu.org/reports/weekly-influenza-bulletin

9. Skowronski DM, Chuang ES, Sabaiduc S, Kaweski SE, Kim S, Dickinson JA, et al. Vaccine effectiveness estimates from an early-season influenza A(H3N2) epidemic, including unique genetic diversity with reassortment, Canada, 2022/23. Euro Surveill. 2023;28:2300043. PubMed https://doi.org/10.2807/1560-7917.ES.2023.28.5.2300043

10. Mercier E, D'Aoust PM, Thakali O, Hegazy N, Jia JJ, Zhang Z, et al. Municipal and neighbourhood level wastewater surveillance and subtyping of an influenza virus outbreak. Sci Rep. 2022;12:15777. PubMed https://doi.org/10.1038/s41598-022-20076-z

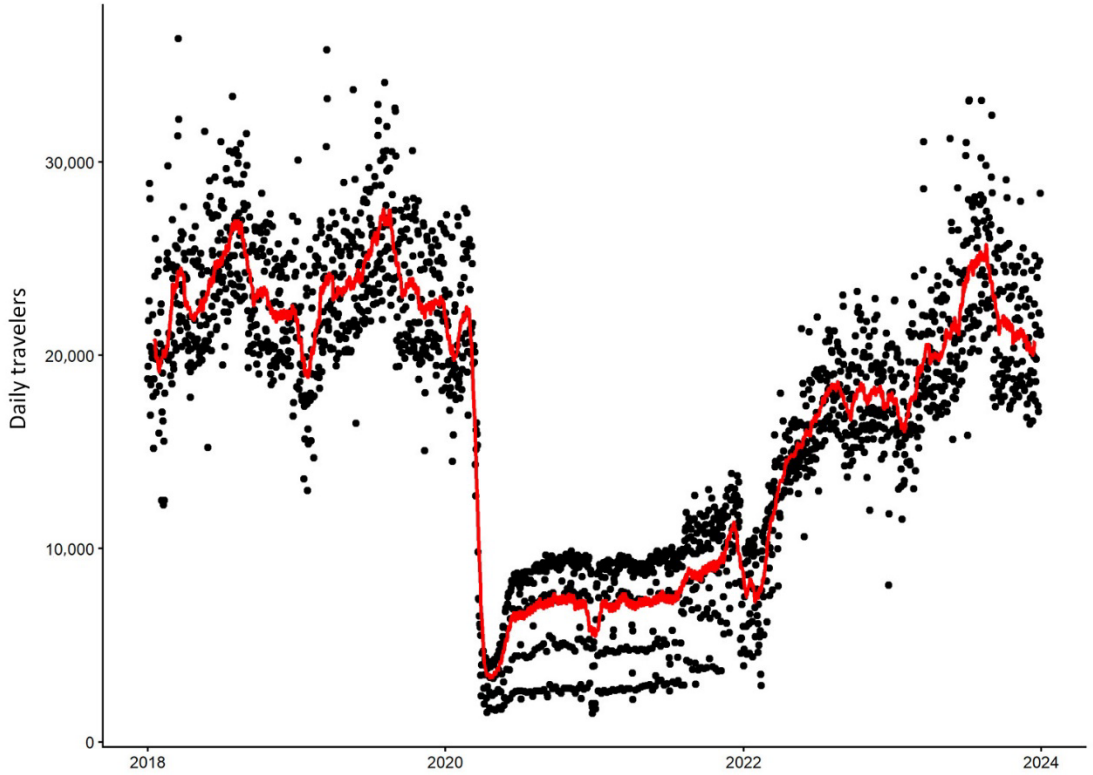

Appendix Figure 1. Daily count of travellers crossing into Windsor-Essex, ON Canada from Detroit at land crossings from January 1, 2018, to December 30, 2023. Dots correspond to the sum of traffic arriving through the Detroit-Windsor tunnel and the Ambassador Bridge. The red line is a 30-day moving average of the daily arrivals. The onset of the COVID-19 pandemic coincides with a precipitous decline in the number of travellers arriving in Windsor-Essex daily. Traveller volume data was publicly available (*7*).

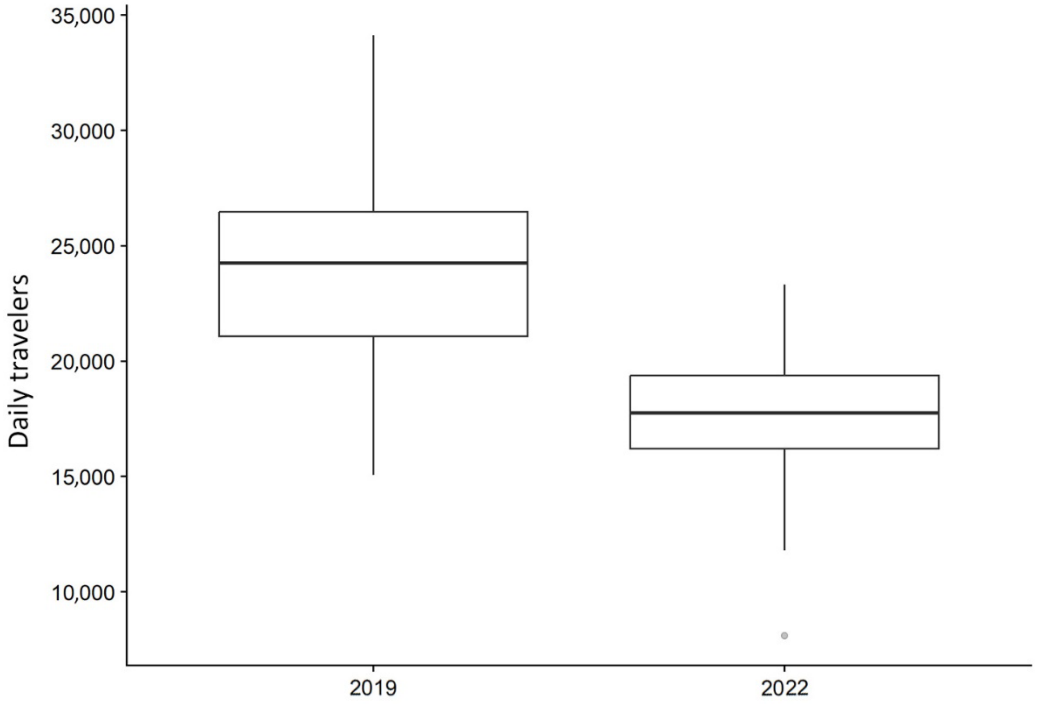

Appendix Figure 2. Comparison of the mean number of daily travellers arriving in Windsor-Essex at land crossings (Detroit-Windsor tunnel and the Ambassador Bridge) from August to December of 2019 (before the COVID-19 pandemic) to the mean number of daily travellers arriving in Windsor-Essex at land crossings from August to December of 2022 (following the removal of COVID-19 pandemic restrictions). The results of a paired *t*-test show that ≈6394 ($p < 0.0001$, 95% CI 5720–7068) fewer daily travellers crossed into Windsor-Essex in 2022 than in the same period of 2019 (a mean of 24,260 travellers in 2019 compared to 17,867 travellers in 2022). This represents an approximate 25% reduction in cross-border traffic during the onset and peak of the 2022–23 respiratory season despite the removal of border restrictions. Traveller volume data were publicly available (*7*).

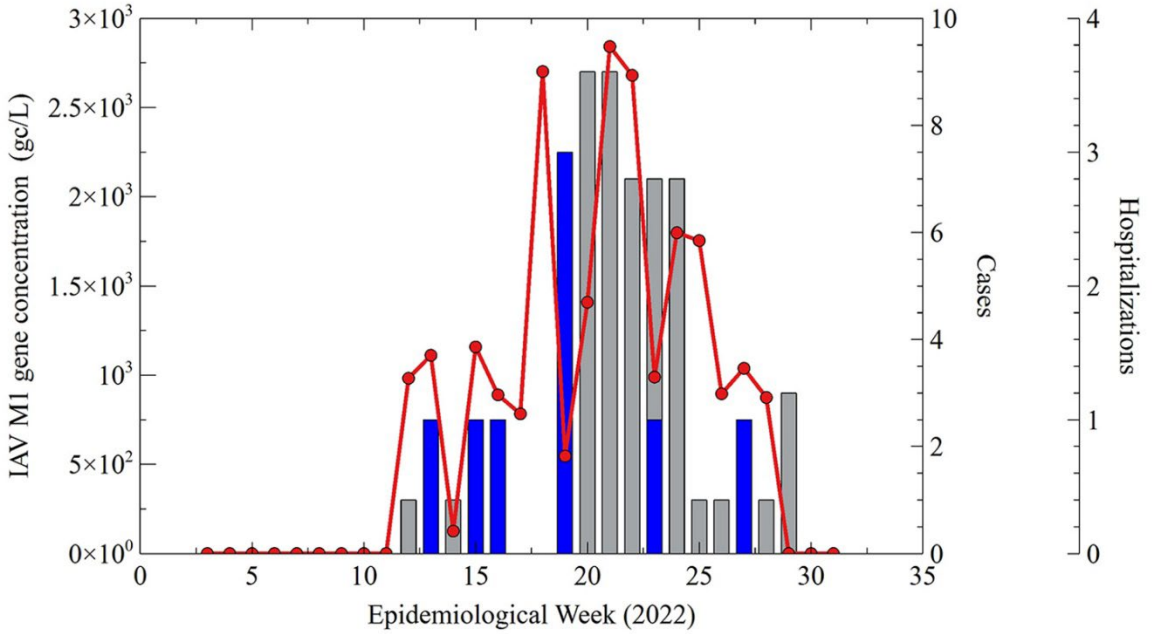

Appendix Figure 3. IAV-M1-gene concentration (red line) superimposed on new influenza hospitalizations for the Windsor-Essex Region (blue bars) and IAV cases (gray bars) per epi-week for 2022. Hospitalization data were extracted from the Discharge Abstract Database (DAD) through IntelliHealth. Influenza hospitalizations included hospital admissions where the main diagnoses had an ICD10 code of J09, J100, J101, J108, J110, J111, or J118. Case data were found on the Windsor-Essex County Health Unit's Public Dashboard (*8*). Unpublished wastewater surveillance data corroborates an abnormal peak in influenza cases and hospitalizations observed in May 2022 following the removal of COVID-19 mitigation measures. This late season spike in influenza circulation was observed across Canada (*9*,*10*).

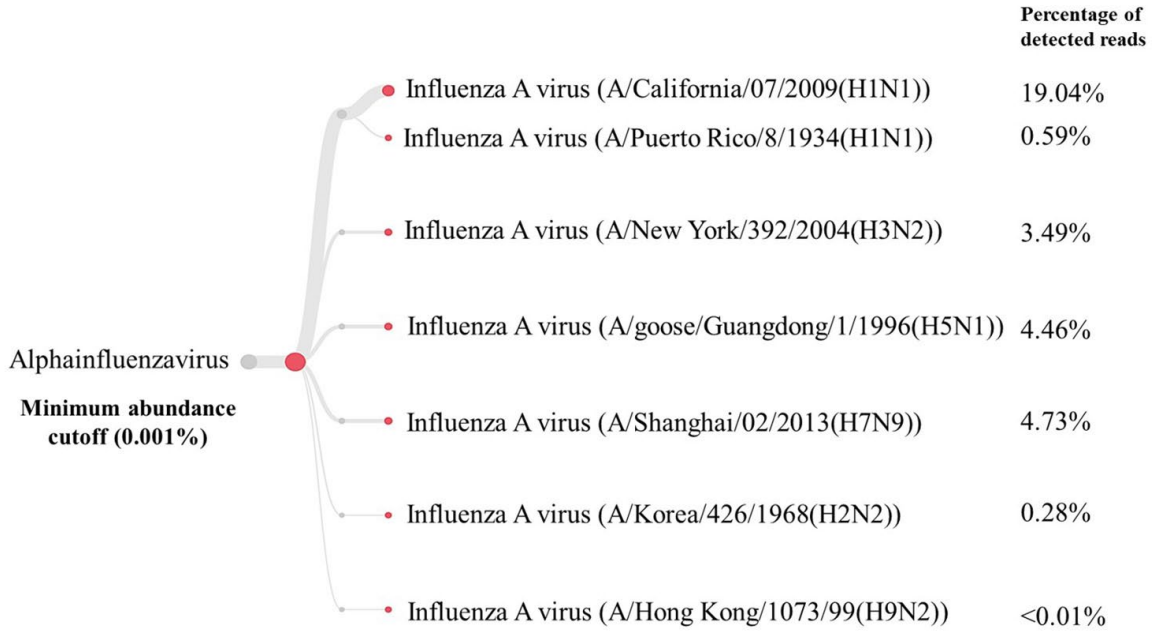

Appendix Figure 4. Taxonomy tree of sequences detected through Nanopore sequencing of the amplicons obtained by RT-qPCR. All the IAV subtypes with at least 0.001% of abundance are included in this taxonomic representation.